THERMODYNAMICS AND CHEMICAL ENGINEERING DATA
Chinese Journal of Chemical Engineering, **17**(5) 781—790 (2009)

Molecular Simulation of CO_2/H_2 Mixture Separation in Metal-organic Frameworks: Effect of Catenation and Electrostatic Interactions*

YANG Qingyuan (阳庆元)[1], **XU Qing** (许青)[1], **LIU Bei** (刘蓓)[2], **ZHONG Chongli** (仲崇立)[1,**] **and Smit Berend**[2]
[1] Lab of Computational Chemistry, Department of Chemical Engineering, Beijing University of Chemical Technology, Beijing 100029, China
[2] Department of Chemical Engineering, University of California, Berkeley, CA 94720-1462, USA

Abstract In this work grand canonical Monte Carlo simulations were performed to study gas separation in three pairs of isoreticular metal-organic frameworks (IRMOFs) with and without catenation at room temperature. Mixture composed of CO_2 and H_2 was selected as the model system to separate. The results show that CO_2 selectivity in catenated MOFs with multi-porous frameworks is much higher than their non-catenated counterparts. The simulations also show that the electrostatic interactions are very important for the selectivity, and the contributions of different electrostatic interactions are different, depending on pore size, pressure and mixture composition. In fact, changing the electrostatic interactions can even qualitatively change the adsorption behavior. A general conclusion is that the electrostatic interactions between adsorbate molecules and the framework atoms play a dominant role at low pressures, and these interactions in catenated MOFs have much more pronounced effects than those in their non-catenated counterparts, while the electrostatic interactions between adsorbate molecules become evident with increasing pressure, and eventually dominant.
Keywords separation, catenation, electrostatic interactions, metal-organic frameworks, molecular simulation

1 INTRODUCTION

Metal-organic frameworks (MOFs) are a novel family of inorganic-organic hybrid porous materials that are formed by the coordination of metal ions with organic linkers. Owing to their fascinating topologies and various potential applications in industrial technologies, the design and synthesis of MOFs has undergone tremendous development in the past decade [1−3]. According to their structural motifs, MOFs can be categorized into two types: those with non-catenated frameworks [4, 5] and others with catenated ones [6, 7]. In the latter additional small pores and adsorption sites are formed by the catenation of frameworks, leading to MOFs with multi-pores of different sizes that may exhibit enhanced gas adsorption and separation properties [8, 9].

One of the main characteristics of MOFs is that although they are neutral, there are always partial charges in framework atoms, resulting in heterogeneous distribution of electrostatic potential in the pores of MOFs. We have identified that in Cu-BTC (benzene-1,3,5-tricarboxylate), one typical non-catenated MOF with two kinds of pores, electrostatic interactions between adsorbate and the framework of Cu-BTC have significant effect on the separation of mixtures where the components have different polarity [10]. However, little is known on the difference in the effects of electrostatic interactions on mixture separation in catenated MOFs and their non-catenated counterparts. This information is difficult to be obtained by experimental methods, while molecular simulation is a powerful method to give insight into the above phenomena at the molecular level [11−17].

In our previous work, it showed that catenated MOFs exhibit high selectivity for the separation of CH_4/H_2 mixture [18], in which the non-bonded interactions were modeled by Lennard-Jones (LJ) potentials, and no electrostatic interactions were needed to be considered. However, for CO or CO_2 separations it is essential to take the electrostatic interactions into account. On the other hand, it seems that the role of electrostatic interactions between adsorbate and the framework of MOF is pore-size dependent, which should be more pronounced in MOFs with small pores. To make this clear, three pairs of MOFs [19], three catenated MOFs and their non-catenated counterparts were adopted in this study to investigate the effect of catenation as well as electrostatic interaction-pore size relationship while excluding the influences of the differences in chemical composition of these materials. Mixture composed of CO_2 and H_2 was selected as the model mixture to separate since this is an important practical system involved in the process of purification of synthetic gas obtained from steam re-forming of natural gas [20].

2 MODELS AND COMPUTATIONAL METHOD

2.1 MOF structures

In this work, six isoreticular metal-organic frameworks (IRMOFs), as synthesized by Eddaoudi *et al*. [19], were adopted as representatives of MOFs. The

Received 2008-12-16, accepted 2009-03-11.
* Supported by the National Natural Science Foundation of China (20725622, 20706002, and 20876006), Beijing Nova Program (2008B15) and the Dutch STW/CW Separation Technology Program (700.56.655-DPC.6243).
** To whom correspondence should be addressed. E-mail: zhongcl@mail.buct.edu.cn

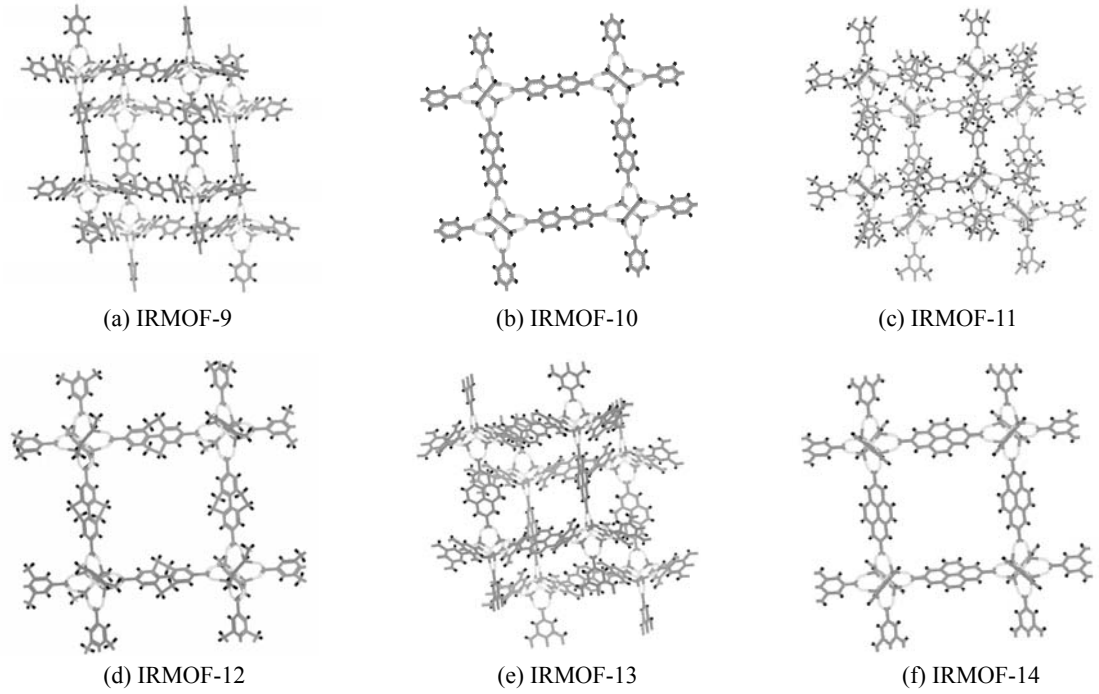

(a) IRMOF-9 (b) IRMOF-10 (c) IRMOF-11

(d) IRMOF-12 (e) IRMOF-13 (f) IRMOF-14

Figure 1 Crystal structures of the IRMOFs used in the simulation

guest-free crystal structures of these IRMOFs were shown in Fig. 1, where IRMOFs-10, 12, and 14 feature the same primitive cubic topology with the octahedral $Zn_4O(CO_2)_6$ clusters linked by different organic dicarboxylate linkers, while IRMOFs-9, 11, and 13 are the catenated counterparts of IRMOFs-10, 12, and 14, respectively.

2.2 Force fields

Force fields play an important role in molecular simulations. In the present work, CO_2 was modeled as a rigid linear molecule with three charged LJ sites located on each atom. A combination of the site-site LJ and Coulombic potentials was used to calculate the CO_2-CO_2 intermolecular interaction. The LJ potential parameters for atom O and C in CO_2 were taken from the TraPPE force field developed by Potoff and Siepmann [21], as listed in Table 1. The C—O bond length is 0.116 nm. In this model, partial point charges centered at each LJ site ($q_O = -0.35$e and $q_C = 0.70$e) approximately represent the first-order electrostatic and second-order induction interactions. Such potential model has been successfully used to simulate the adsorption of CO_2 in zeolites [22] and MOF materials [10, 11, 13].

H_2 was treated as a diatomic molecule modeled by a LJ core located at its center of mass and three partial charges with two ($q = 0.468$e) located at H atoms and one ($q = -0.936$e) at the center between two H atoms. The interactions between various sites in the adsorbed molecules were also calculated by the summation of LJ interactions and the electrostatic interactions. The LJ parameters for hydrogen molecule were taken from the force field suggested by Marx and Nielaba [23], as shown in Table 1. The bond length between two H atoms in molecule is 0.074 nm. These parameters have been successfully adopted to predict the adsorption of hydrogen in carbon nanohorns [24] and MOFs [11, 12].

Table 1 LJ potential parameters for CO_2, H_2, and the IRMOFs used in this work

LJ parameters	σ/nm	(ε/k_B)/K
CO_2_C	0.280	27.0
CO_2_O	0.305	79.0
H_2	0.296	36.7
MOF_O	0.312	30.19
MOF_C	0.343	52.84
MOF_H	0.257	22.14
MOF_Zn	0.246	62.40

For the IRMOFs studied here, a combination of the site-site LJ and Coulombic potentials was also used to calculate the interactions between adsorbate molecules and adsorbents. The LJ parameters for the framework atoms in the IRMOFs were taken from the universal force field (UFF) of Rappe *et al*. [25], which has been successfully employed to depict the adsorption of several light gases and their mixtures in MOFs [12, 16−18]. The potential parameters used in this work are listed in Table 1. All the LJ cross interaction parameters were determined by the Lorentz-Berthelot mixing rules in our simulations.

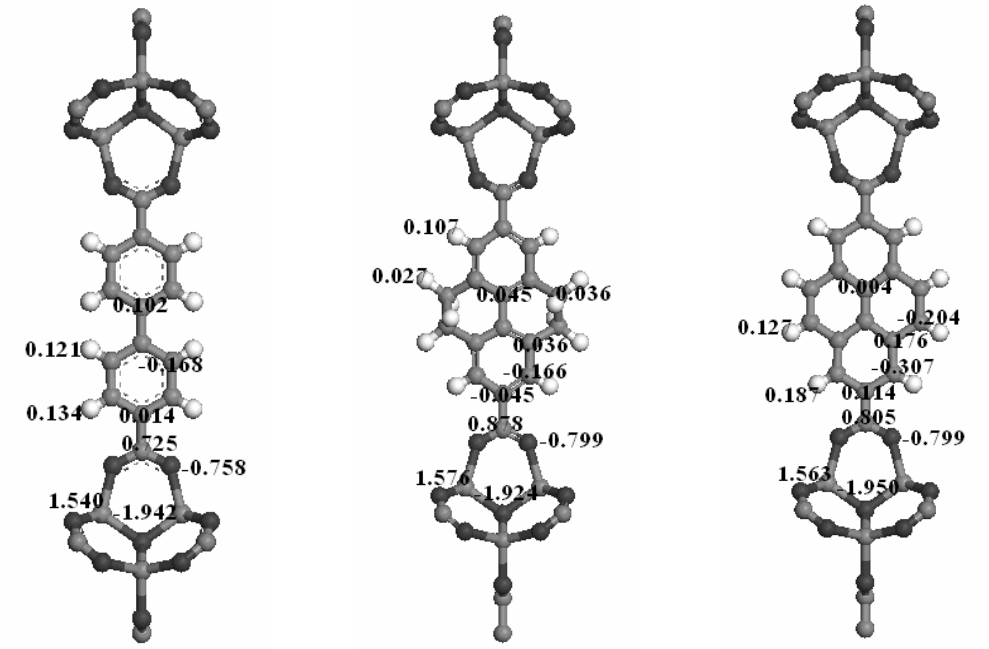

(a) IRMOF-9 and 10 (b) IRMOF-11 and 12 (c) IRMOF-13 and 14

Figure 2 Model clusters of the MOFs used in the calculations of atomic partial charges

The atomic partial charges for the atoms in IRMOFs-10, 12, and 14 were taken from our previous work [13], which were obtained from the density functional theory (DFT) calculations using unrestricted B3LYP functional and ChelpG method. Details of the DFT calculations can be found elsewhere [13]. Since the atomic partial charge presented in an atom of a framework is mainly determined by the atoms bonded to it, it is a good approximation to treat the catenated IRMOFs-9, 11, and 13 to have identical atomic partial charges to their corresponding non-catenated counterparts IRMOFs-10, 12, and 14. The cluster models used for DFT calculations together with the obtained atomic partial charges are shown in Fig. 2.

The adsorption isotherms of pure CO_2 and H_2 in IRMOF-1 (MOF-5) were simulated and compared with experimental data at 298 K as shown in Fig. 3 to further confirm the reliability of the above set of force fields adopted in this work. The results shown in Fig. 3 (a) indicate that the simulations enable excellent reproduction of the experimental adsorption isotherm of CO_2 [26] over the entire pressure range, while excellent agreement between simulation and experiment [27] was obtained up to 2 MPa for H_2 as shown in Fig. 3 (b). This is caused by the fact that the small excess values measured at 298 K are inherently more susceptible to the effects of experimental and statistical error. Thus, the error between the experimental results and the simulations could be due to our standard method of calculating excess adsorption from absolute adsorption compared to the experimental procedures for system calibration and measurement of the excess isotherms. Similar agreement has been reached for a slightly different potential by Frost and Snurr [28], and

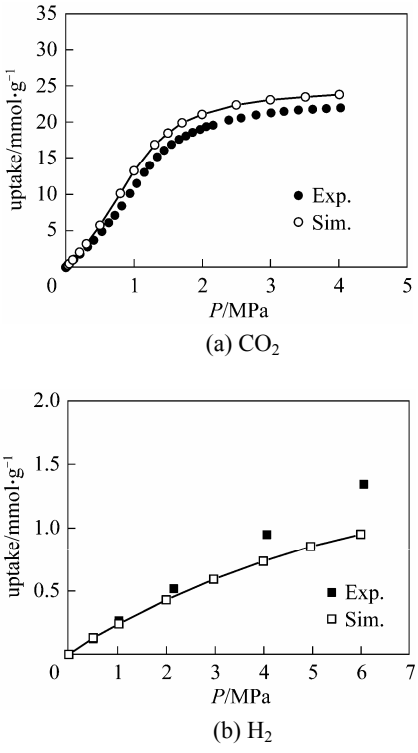

Figure 3 Comparison of simulated and experimental [26, 27] isotherms of CO_2 and H_2 in IRMOF-1 (MOF-5) at 298 K

reasonable agreements were obtained at 77 K by them using the same potential model. Therefore, the force fields adopted in this work are reliable to investigate the adsorption behaviors of CO_2/H_2 mixture in IRMOFs

with pressures up to 2 MPa.

2.3 Simulation method

Grand canonical Monte Carlo (GCMC) simulations were employed to calculate the adsorption of pure components and their mixtures in all studied IRMOFs. Details on the method can be found elsewhere [29]. The adsorption simulations were investigated at 298 K. Peng-Robinson equation of state was used to relate the bulk pressure with chemical potential required in the GCMC simulations. Similar to previous works [10−18], all the IRMOFs were treated as rigid frameworks with atoms frozen at their crystallographic positions during simulations. The simulation box representing IRMOF-9 contained 12 (3×2×2) unit cells, while 8 (2×2×2) unit cells were adopted for other MOFs. The simulations with larger boxes showed that no finite-size effects existed using the above boxes. A cutoff radius of 1.3 nm was applied to all the LJ interactions, and the long-range electrostatic interactions were handled using the Ewald summation technique. Periodic boundary conditions were applied in all three dimensions. Since the adsorbent was assumed to be a rigid structure, the potential energies between an adsorbate and the adsorbent were initially tabulated on a series of three dimensional grid points with grid space of 0.015 nm. During the simulations, the potential energy at any position in the adsorbent was determined by interpolation [10−13]. For each state point, GCMC simulation consisted of 1.5×10^7 steps to guarantee the equilibration, followed by 1.5×10^7 steps to sample the desired thermodynamic properties.

3 RESULTS AND DISCUSSION

3.1 Effect of catenation on adsorption selectivity

As the first step, molecular simulations were performed to calculate the adsorption selectivity of CO_2 from the binary mixtures of CO_2/H_2 in the three catenated IRMOFs as well as their non-catenated counterparts. In separation processes a good indication of the ability for separation is the selectivity of a porous material for different components in mixtures. The selectivity for component A relative to component B is defined by $S=(x_A/x_B)(y_B/y_A)$, where x_A and x_B are the mole fractions of components A and B in the adsorbed phase, while y_A and y_B are the mole fractions of components A and B in the bulk phase, respectively.

The simulated adsorption selectivity of CO_2 from binary mixture of CO_2/H_2 with five gas compositions at 298 K are shown in Fig. 4, as a function of the bulk pressure up to 2.0 MPa. Clearly, the adsorption selectivity behaves much differently in the two types of IRMOFs. As can be seen from Fig. 4, the adsorption selectivities for CO_2 in the IRMOFs (IRMOF-9, IRMOF-11, and IRMOF-13) with catenation are much higher than those in their corresponding non-catenated counterparts (IRMOF-10, IRMOF-12, and IRMOF-14,

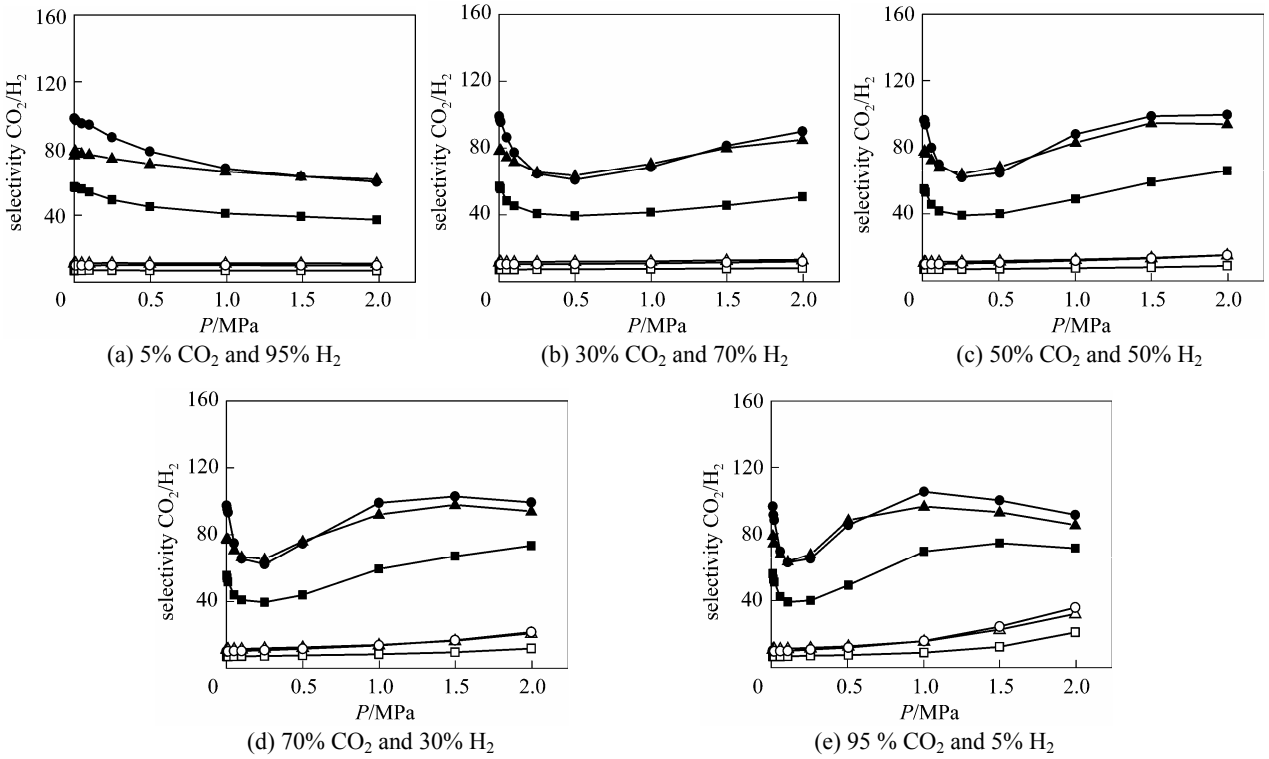

Figure 4 Selectivity for CO_2 from CO_2/H_2 mixtures with various gas compositions at 298 K
■ IRMOF-9; □ IRMOF-10; ▲ IRMOF-11; △ IRMOF-12; ● IRMOF-13; ○ IRMOF-14

respectively), indicating that catenation can significantly improve the adsorption selectivity for CO_2/H_2 system, which has also been observed for the separation of CH_4/H_2 mixture in these materials [18]. Fig. 4 also shows that the selectivities in IRMOF-11 and IRMOF-13 are higher than that in IRMOF-9, which is caused mainly by the different modes of catenation in their crystal structures. In IRMOF-11 or -13 the two separate frameworks are interwoven such that there is minimal distance between them without atomic overlap, while IRMOF-9 maximizes the distance between the two separate frameworks. Thus, the interwoven IRMOF-11 (or -13) has deeper interaction potential for CO_2 molecules than that in the interpenetrated IRMOF-9, resulting in larger selectivity as shown in Fig. 4.

Separation of equimolar mixture of CO_2/H_2 has been performed in other porous materials, for example, the selectivity is 45.0 in activated carbon [30] and 3.5 in microporous silica membrane [31] at room temperature and moderate pressure ($T = 298$ K and $P = 2.0$ MPa). In addition, in the low-pressure limit the selectivity is 70.65 in zeolites Na-4A for mixture with composition $CO_2 : H_2 = 98.6 : 1.4$ [32]. Thus, Fig. 4 demonstrates that the generation of catenated structures is a promising strategy to produce MOF materials for separation applications.

Figure 4 also shows that the pressure dependency of the adsorption selectivity is very different in the two types of materials, *i.e*. the non-catenated IRMOFs and their catenated counterparts. For IRMOF-10, IRMOF-12, and IRMOF-14, the selectivity of CO_2 within the pressure range studied is nearly pressure-independent for CO_2 compositions less than 50%. When the composition exceeds this value, the selectivity gradually increases with increasing pressure, and this trend becomes more evident at higher CO_2 compositions. As CO_2 and H_2 differ significantly in size, one would expect, because of entropic reasons, the smaller molecule to be preferentially adsorbed. However, at the conditions of the simulations there is still much free space in the non-catenated IRMOF's and one would therefore expect to see a selectivity reversal at much higher pressures. Thus, the interactions involved by CO_2 molecules are dominant for the adsorption selectivity within the simulated pressure range.

As to IRMOF-9, IRMOF-11, and IRMOF-13 with catenated structures, the selectivity behavior is much more complicated; nevertheless, a common trend exists in all the examined gas compositions: first a rapid decrease of selectivity is observed for low pressures, which becomes more pronounced with increasing CO_2 composition. This decrease can be attributed to the fact that, in the catenated IRMOFs there are different types of pores (4 in IRMOF-9, 6 in IRMOF-11, and 5 in IRMOF-13) with much smaller sizes, leading to stronger confinement effects in the catenated small pore space, and thus packing effects become evident at low pressures. Due to the same reason, Fig. 4 shows that the trends of selectivity in the catenated IRMOFs are very sensitive to CO_2 composition as well as the bulk pressure. In addition, when CO_2 compositions are not too low, the interactions involved by CO_2 molecules are strong at higher pressures, causing a second step of selectivity increasing as shown in Figs. 4 (b−e). Detailed discussions on how these interactions influence the CO_2 selectivity behavior will be given in the next part. In addition, with further increasing pressure, the larger pore space in MOFs with catenated structures are almost filled up, and the entropic effects of H_2 molecules with smaller molecular size become predominant, which again results in the decreasing trend as shown in Figs. 4 (c−e). Similar behavior has also been observed in our previous work for the separation of CO_2/H_2 mixture in Cu-BTC, which has two kinds of small-size pores [11]. Fig. 4 also shows that, the selectivities in IRMOF-11 and IRMOF-13 are very close due to their similar structures, which is also the case for IRMOF-12 and IRMOF-14.

3.2 Effect of various electrostatic interactions

There exist two kinds of interactions: the van der Waals and electrostatic interactions for the systems studied in this work. Since one of the main characteristics of MOFs is that there are atomic partial charges in the atoms of the frameworks, it is interesting to study how the electrostatic interactions influence the selectivity behavior of gas mixtures. Therefore, we performed a systematic study on the effects of various electrostatic interactions on CO_2 selectivity.

Firstly, we switch off all the electrostatic interactions in the systems, and the simulation results for CO_2/H_2 mixture with two gas compositions (50% CO_2 and 50% H_2; 95 % CO_2 and 5% H_2) at 298 K are shown in Fig. 5. Compared with the results shown in Figs. 4 (c and e), Fig. 5 shows that the selectivity of CO_2 from CO_2/H_2 mixture does not show the increasing selectivity with increasing pressure. Therefore, the remarkable increase in the selectivity at higher pressures shown in Figs. 4(b−e) is caused by the electrostatic interactions.

To further understand whether this effect is due to the electrostatic interactions between the adsorbed molecules or between the adsorbed molecules and the atoms of the IRMOFs, two additional GCMC simulations were performed for CO_2/H_2 mixture with equimolar gas composition: case 2, in which we only switch off the electrostatic interactions of adsorbates-IRMOFs, and case 3, in which we switch off the electrostatic interactions between adsorbate molecules. The simulated results in IRMOF-9 and IRMOF-10 are given as an example in Fig. 6. The results for all of the electrostatic interactions are switched off (denoted as case 1) as well as those are all considered (denoted as case 4) are also included in Fig. 6 for comparison.

As can be seen from Fig. 6 (a), the effects of various contributions to electrostatic interactions on the selectivity depend on the pressure. At low pressures, the amount of molecules adsorbed in the material is very small, and the effects of the electrostatic

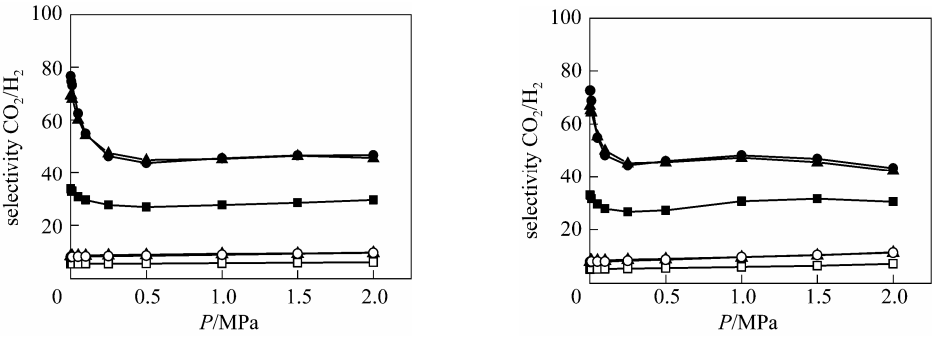

Figure 5 The simulated selectivity of CO_2 from CO_2/H_2 mixture without considering any electrostatic interactions in system at 298 K

■ IRMOF-9; □ IRMOF-10; ▲ IRMOF-11; △ IRMOF-12; ● IRMOF-13; ○ IRMOF-14

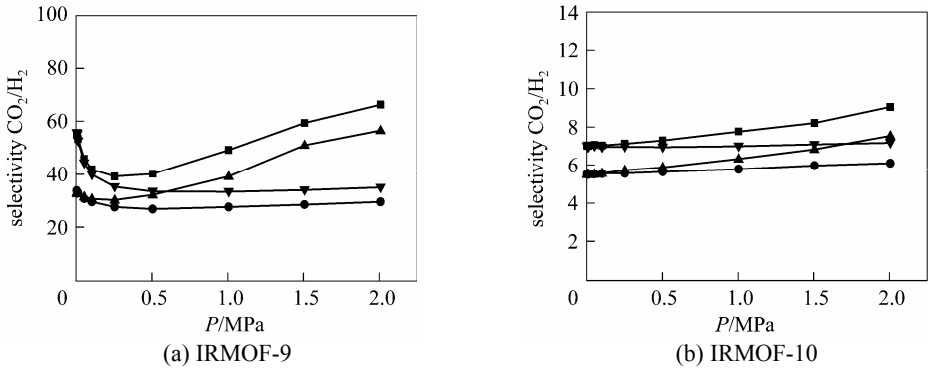

Figure 6 Effects of the various electrostatic interactions on the selectivity of CO_2 from equimolar mixture of CO_2/H_2 at 298 K in IRMOF-9 and IRMOF-10

● case 1; ▲ case 2; ▼ case 3; ■ case 4

interactions between adsorbed molecules on the selectivity are negligible, which explains the identical selectivities in cases 1 and 2. On the other hand, the electrostatic interactions between the adsorbate molecules and the framework atoms in IRMOF-9 can greatly enhance the selectivity of CO_2 from CO_2/H_2 mixture at low pressures (selectivity changes from 33 to 55). It is found that the effect of the electrostatic interactions involved by H_2 molecules on its adsorption are very small at room temperature, which was also observed by Garberoglio *et al* [12]. Thus, the enhanced selectivity at low pressures can be explained by the electrostatic interactions between CO_2-IRMOFs. In addition, Fig. 6 also shows that at low pressures the effect of electrostatic interactions between CO_2- IRMOFs on selectivity is much more pronounced in catenated MOFs than that in their non-catenated counterparts.

It is also found from Fig. 6 that with increasing pressure the selectivities in cases 1 and 3, where the electrostatic interactions between adsorbate molecules are not considered, do not exhibit an increasing selectivity at higher pressures. However, when only the electrostatic interactions between adsorbate molecules are considered (case 2), the selectivity shows a significant increase for pressure larger than 0.25 MPa. The above analysis indicated that the electrostatic interactions between CO_2 molecules dominantly enhance the selectivity at higher pressures, which results in the remarkable increase in the selectivity at higher pressures as shown in Figs. 4 (b)−(e). Fig. 6 (b) shows that the above points also hold for IRMOF-10. The selectivities in other studied IRMOFs show similar behaviors in the four cases.

The separation behavior of CO_2/CH_4 mixture in Cu-BTC under cases 2 and 4 in our previous work [10] was also examined. For case 2 with only the electrostatic interactions between adsorbates-frameworks being switched off, the trends in selectivity are similar in the separation of CO_2/CH_4 mixture in Cu-BTC and CO_2/H_2 mixture in the catenated IRMOFs. However, when all of the electrostatic interactions in systems are considered (case 4), the first rapid decrease in selectivity at low pressure for CO_2/H_2 mixture in IRMOF-9 was not observed for CO_2/CH_4 mixture separation in Cu-BTC. This difference could be explained by two reasons. First, there are multi-pores with different sizes in catenated IRMOFs, while only two kinds of pores exist in non-catenated Cu-BTC, which causes the molecular occupations are much more complex in the former. Another reason is that the difference in the molecular size is much larger between CO_2 and H_2 molecules than that between CO_2 and CH_4 molecules, and this causes a greater entropic effect for H_2 molecules

during CO_2/H_2 co-adsorption in catenated IRMOFs with multiple small pores.

To visualize the effect of the electrostatic interactions between adsorbates-IRMOFs, the center of mass (COM) probability distributions of adsorbed CO_2 and H_2 molecules were compared in cases 2 and 4 at 0.1 MPa. To do this, the unit cell of material was first divided into many small cubic grids with grid length of 0.128 nm; then the occupying times of the COM of molecules in each grid were counted during simulation; and at the end of simulation, the statistical probability distribution of each species in each grid was obtained with the occupying times divided by the product of total accumulated molecules of the corresponding species, the simulation steps and grid volume. Finally, the averaged probability distributions were obtained by adding the probability together in grids between the examined narrow gaps along one visual direction. Fig. 7 shows the probability distribution plots of COM densities of adsorbed molecules in IRMOF-9 for a CO_2/H_2 mixture with equimolar composition along x direction. Figs. 7 (a) and (b) illustrate that, where only the COM probability densities of CO_2 are given, electrostatic interactions between CO_2-IRMOF-9 present significant effects on the COM probability distribution at low pressure. The COM probability density plots of H_2 are shown in Figs. 7 (c) and (d), in which CO_2 molecules are omitted for clarity. Obviously, the COM distribution of H_2 molecules is almost unaffected due to the very weak electrostatic interactions for them with IRMOF-9. In addition, these results indicate that the largest effect of electrostatic interactions on the selectivity occurs in the small pores formed by catenation. For comparison, Fig. 8 shows the probability distribution plots of the COM densities of this mixture in non-catenated IRMOF-10. Obviously, similar tendency on the effect of electrostatic interactions were observed, however, due to the larger pore size in IRMOF-10, the effect of electrostatic interactions between adsorbates and IRMOF-10 is much weaker than that in IRMOF-9, and the largest effect on the selectivity occurs around the $Zn_4O(CO_2)_6$ clusters in non-catenated IRMOF-10.

3.3 Effect of catenation on local selectivity

The selectivity discussed above is the total performance of IRMOFs for the separation of CO_2/H_2 mixtures. However, due to the complexity in the structures of these materials, the selectivity as well as the effect of electrostatic interactions between adsorbates-IRMOFs should be differently distributed in various local regions of these materials, especially in catenated IRMOFs. As discussed above, the electrostatic interactions between CO_2-IRMOFs dominantly enhance the selectivity at low pressures. Thus, the corresponding local selectivity in catenated IRMOF-9 and IRMOF-10 at 0.1 MPa were calculated and the results are presented in Fig. 9 to give a clearer picture for the results shown in Figs. 7 and 8.

The calculated results shown in Fig. 9 clearly

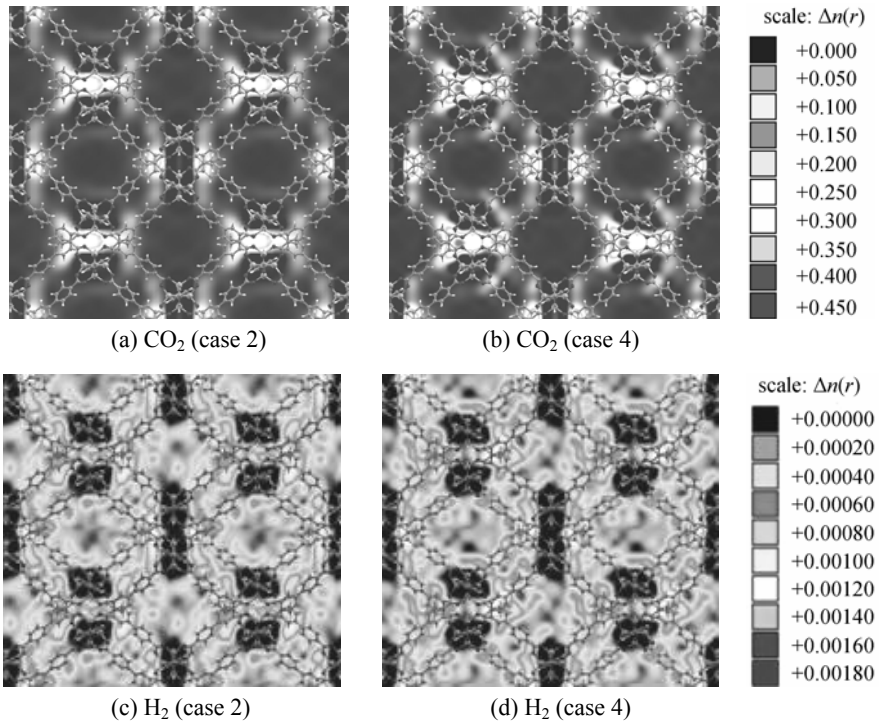

Figure 7 Probability distribution plots of COM densities of adsorbed CO_2 (a, b) and H_2 (c, d) molecules in planes through the catenated area in IRMOF-9 at 298 K and 0.1 MPa

(Case 2: only switching off the electrostatic interactions between adsorbates-IRMOF-9; case 4: considering all the electrostatic interactions)

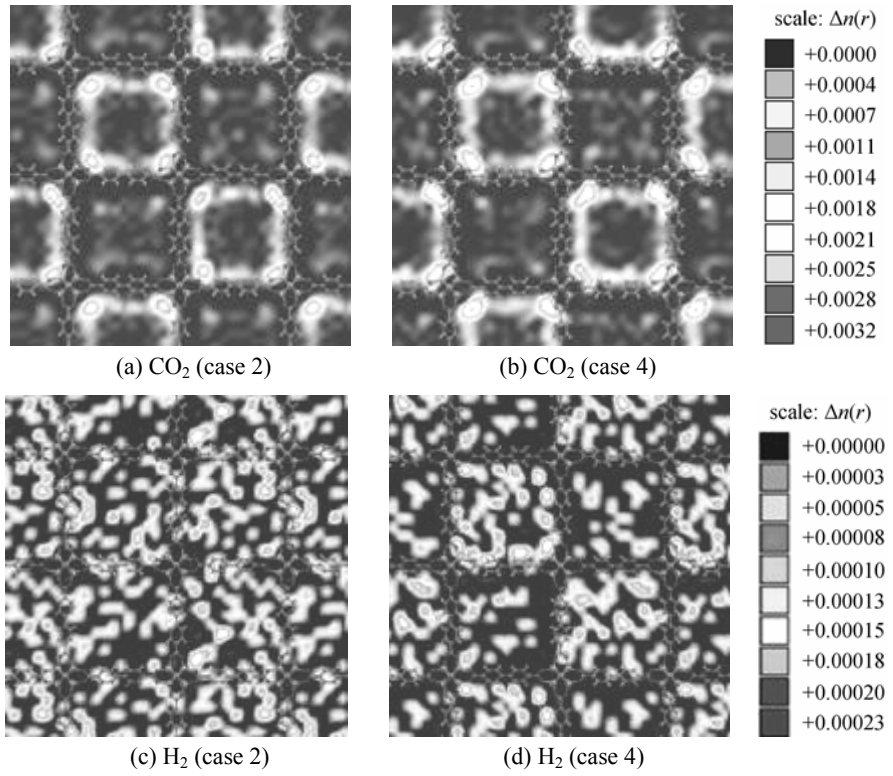

(a) CO_2 (case 2) (b) CO_2 (case 4)

(c) H_2 (case 2) (d) H_2 (case 4)

Figure 8 Probability distribution plots of the COM densities of adsorbed CO_2 (a, b) and H_2 (c, d) molecules in planes through the $Zn_4O(CO_2)_6$ cluster area in IRMOF-10 at 298 K and 0.1 MPa
(Case 2: only switching off the electrostatic interactions between adsorbates-IRMOF-10; case 4: considering all the electrostatic interactions)

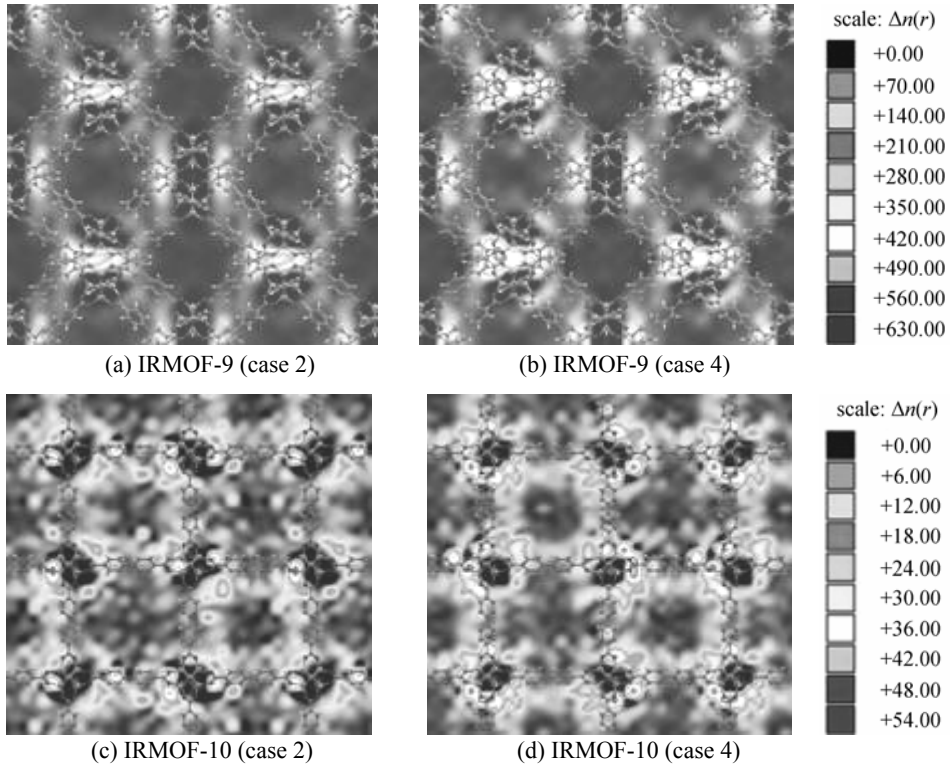

(a) IRMOF-9 (case 2) (b) IRMOF-9 (case 4)

(c) IRMOF-10 (case 2) (d) IRMOF-10 (case 4)

Figure 9 Selectivity distribution of CO_2 from equimolar mixture of CO_2/H_2 in planes through the catenated area in IRMOF-9 (a, b) and through the $Zn_4O(CO_2)_6$ cluster area in IRMOF-10 (c, d) at 298 K and 0.1 MPa
(Case 2: only switching off the electrostatic interactions between adsorbates-IRMOFs; case 4: considering all the electrostatic interactions)

demonstrate that the electrostatic interactions between adsorbate-framework mainly contribute to the selectivity enhancement at low pressure. The effect of these interactions on the local selectivity in catenated IRMOF-9 is much more significant than those in non-catenated IRMOF-10, which is in good agreement with the COM distributions illustrated in Figs. 7 and 8. Furthermore, Fig. 9 also shows that the highest effect of electrostatic interactions occurs in the small pores formed by two metal clusters and phenyl linkers in IRMOF-9, while for IRMOF-10 the most pronounced effect occurs around the $Zn_4O(CO_2)_6$ clusters. On the other hand, it also can be found in Fig. 9 that the local selectivities in the catenated area of IRMOF-9 are much higher than those around the $Zn_4O(CO_2)_6$ clusters in non-catenated IRMOF-10.

4 CONCLUSIONS

This work shows that catenation can greatly enhance the selectivity of CO_2 from CO_2/H_2 mixtures in MOFs due to the presence of various small pores with different sizes, and the electrostatic interactions play a key role in selectivity enhancement. However, the contributions are different for different parts, depending on pore size, pressure, and composition. Generally, the electrostatic interactions between adsorbate molecules and the framework atoms play a dominant role at low pressures, and the effect of these interactions in catenated MOFs is much more pronounced than that in their non-catenated counterparts due to the presence of various small pores. Thus, the role of the electrostatic interactions between adsorbate and MOF is significantly affected by pore size. With increasing pressure the role of the electrostatic interactions between adsorbate molecules becomes more evident and eventually dominant. The electrostatic interactions do not only change the values of selectivity but also can even change the trend of selectivity behavior for MOFs with small pores. Thus, it is an important property to be considered in material screening and applications.

REFERENCES

1 Férey, G., "Hybrid porous solids: Past, present, future", *Chem. Soc. Rev.*, **37**, 191−214 (2008).

2 Siberio-Pérez, D.Y., Wong-Foy, A.G., Yaghi, O.M., Matzger, A.J., "Raman spectroscopic investigation of CH_4 and N_2 adsorption in metal-organic frameworks", *Chem. Mater.*, **19**, 3681−3685 (2007).

3 Ma, S., Sun, D.F., Simmons, J.M., Collier, C.D., Yuan, D., Zhou, H.C., "Metal-organic framework from an anthracene derivative containing nanoscopic cages exhibiting high methane uptake", *J. Am. Chem. Soc.*, **130**, 1012−1016 (2008).

4 Hwang, Y.K., Hong, D.Y., Chang, J.S., Jhung, S.H., Seo, Y.K., Kim, J., Vimont, A., Daturi, M., Serre, C., Férey, G. "Amine grafting on coordinatively unsaturated metal centers of MOFs: Consequences for catalysis and metal encapsulation", *Angew. Chem. Int. Ed.*, **47**, 4144−4148 (2008).

5 Banerjee, R., Phan, A., Wang, B., Knobler, C., Furukawa, H., O'Keeffe, M., Yaghi, O.M., "High-throughput synthesis of zeolitic imidazolate frameworks and application to CO_2 capture", *Science*, **319**, 939−943 (2008).

6 Chen, B.L., Ma, S.Q., Hurtado, E.J., Lobkovsky, E.B., Zhou, H.C., "A triply interpenetrated microporous metal-organic framework for selective sorption of gas molecules", *Inorg. Chem.*, **46**, 8490−8492 (2007).

7 Zhang, J.P., Kitagawa, S., "Supramolecular isomerism, framework flexibility, unsaturated metal center, and porous property of Ag(I)/Cu(I) 3,3′,5,5′-tetrametyl-4,4′-bipyrazolate", *J. Am. Chem. Soc.*, **130**, 907−917 (2008).

8 Ma, S.Q., Sun, D.F., Ambrogio, M., Fillinger, J.A., Parkin, S., Zhou, H.C., "Framework-catenation isomerism in metal-organic frameworks and its impact on hydrogen uptake", *J. Am. Chem. Soc.*, **129**, 1858−1859 (2007).

9 Bastin, L., Bárcia, P.S., Hurtado, E.J., Silva, J.A.C., Rodrigues, A.E., Chen, B., "A microporous metal-organic framework for separation of CO_2/N_2 and CO_2/CH_4 by fixed-bed adsorption", *J. Phys. Chem. C*, **112**, 1575−1581 (2008).

10 Yang, Q.Y., Zhong, C.L., "Electrostatic-field-induced enhancement of gas mixture separation in metal-organic frameworks: A computational study", *Chem. Phys. Chem.*, **7**, 1417−1421 (2006).

11 Yang, Q.Y., Zhong, C.L., "Molecular simulation of carbon dioxide/methane/hydrogen mixture adsorption in metal-organic frameworks", *J. Phys. Chem. B*, **110**, 17776−17783 (2006).

12 Garberoglio, G., Skoulidas, A. I., Johnson, J. K., "Adsorption of gases in metal organic materials: Comparison of simulations and experiments", *J. Phys. Chem. B*, **109**, 13094−13103 (2005).

13 Yang, Q.Y., Zhong, C.L., "Computational study of CO_2 storage in metal-organic frameworks", *J. Phys. Chem. C*, **112**, 1562−1569 (2008).

14 Ramsahye, N.A., Maurin, G., Bourrelly, S., Llewellyn, P.L., Serre, C., Loiseau, T., Devic, T., Ferey, G., "Probing the adsorption sites for CO_2 in metal organic frameworks materials MIL-53 (Al, Cr) and MIL-47 (V) by density functional theory", *J. Phys. Chem. C*, **112**, 514−520 (2008).

15 Walton, K.S., Millward, A.R., Dubbeldam, D., Frost, H., Low, J.J., Yaghi, O.M., Snurr, R.Q., "Understanding inflections and steps in carbon dioxide adsorption isotherms in metal-organic frameworks", *J. Am. Chem. Soc.*, **130**, 406−407 (2008).

16 Babarao, R., Hu, Z., Jiang, J., Chempath, S., Sandler, S.I., "Storage and separation of CO_2 and CH_4 in silicalite, C_{168} schwatzite, and IRMOF-1: A comparative study from Monte Carlo simulation", *Langmuir*, **23**, 659−666 (2007).

17 Keskin, S., Sholl, D.S., "Screening metal-organic framework materials for membrane-based methane/carbon dioxide separations", *J. Phys. Chem. C*, **111**, 14055−14059 (2007).

18 Liu, B., Yang, Q.Y., Xue, C.Y., Zhong, C.L., Chen, B.H., Smit, B., "Enhanced adsorption selectivity of hydrogen/methane mixtures in metal-organic frameworks with interpenetration: A molecular simulation study", *J. Phys. Chem. C*, **112**, 9854−9860 (2008).

19 Eddaoudi, M., Kim, J., Rosi, N., Vodak, D., Wachter, J., O'Keeffe, M., Yaghi, O.M., "Systematic design of pore size and functionality in isoreticular MOFs and their application in methane storage", *Science*, **295**, 469−472 (2002).

20 Mitchell, M.C., Gallo, M., Nenoff, T.M., "Molecular dynamics simulations of binary mixtures of methane and hydrogen in titanosilicates", *J. Chem. Phys.*, **121**, 1910−1916 (2004).

21 Potoff, J.J., Siepmann, J.I., "Vapor-liquid equilibria of mixtures containing alkanes, carbon dioxide, and nitrogen", *AIChE J.*, **47**, 1676−1682 (2001).

22 Goj, A., Sholl, D.S., Akten, E.D., Kohen, D., "Atomistic simulations

of CO_2 and N_2 adsorption in silica zeolites: The impact of pore size and shape", *J. Phys. Chem. B*, **106**, 8367−8375 (2002).

23 Marx, D., Nielaba, P., "Path-integral Monte Carlo techniques for rotational motion in two dimensions: Quenched, annealed, and no-spin quantum-statistical averages", *Phys. Rev. A*, **45**, 8968−8971 (1994).

24 Tanaka, H., Kanoh, H., Yudasaka, M., Iijima, S., Kaneko, K. "Quantum effects on hydrogen isotope adsorption on single-wall carbon nanohorns", *J. Am. Chem. Soc.*, **127**, 7511−7516 (2005).

25 Rappe, A.K., Casewit, C.J., Colwell, K.S., Goddard III, W.A., Skiff, W.M., " UFF, a full periodic table force field for molecular mechanics and molecular dynamics simulations", *J. Am. Chem. Soc.*, **114**, 10024−10035 (1992).

26 Millward, A.R., Yaghi, O.M., "Metal-organic frameworks with exceptionally high capacity for storage of carbon dioxide at room temperature", *J. Am. Chem. Soc.*, **127**, 17998−17999 (2005).

27 Li, Y., Yang, R.T., "Hydrogen storage in metal-organic frameworks by bridged hydrogen spillover", *J. Am. Chem. Soc.*, **128**, 8136−8137 (2006).

28 Frost, H., Snurr, R.Q., "Design requirements for metal-organic frameworks as hydrogen storage materials", *J. Phys. Chem. C*, **111**, 18794−18803 (2007).

29 Frenkel, D., Smit, B., Understanding Molecular Simulation: From Algorithms to Applications, Academic Press, San Diego, CA (2002).

30 Cao, D.P., Wu, J.Z., "Modeling the selectivity of activated carbons for efficient separation of hydrogen and carbon dioxide", *Carbon*, **43**, 1364−1370 (2005).

31 Richard, V., Favre, E., Tondur, D., Nijmeijer, A., "Experimental study of hydrogen, carbon dioxide and nitrogen permeation through a microporous silica membrane", *Chem. Eng. J.*, **84**, 593−598 (2001).

32 Akten, E.D., Siriwardane, R., Sholl, D.S., "Monte Carlo simulation of single- and binary-component adsorption of CO_2, N_2, and H_2 in zeolite Na-4A", *Energy & Fuel*, **17**, 977−983 (2003).